ADVANCES IN MATERIALS SCIENCE, Vol. 20, No. 3(65), September 2020

DOI : 10.2478/adms-2020-0017

B. Maaoui[a,b], Y. Aoun[a]*, S. Benramache[c], A. Nid[a], R. Far[a], A. Touati[a]

[a] *Mechanical Department, Faculty of Technology, University of El-Oued, El-Oued 39000, Algeria*

[b] *VTRS Laboratory, Institute of Technology, University of El-Oued, El-Oued 39000, Algeria*

[c] *Material Sciences Department, University of Biskra, Biskra 07000, Algeria*

** aounyacine07@gmail.com*

SYNTHESIS AND CHARACTERIZATION OF PHYSICAL PROPERTIES OF THE NiO THIN FILMS BY VARIOUS CONCENTRATIONS

ABSTRACT

In this work, nickel oxide was deposited on a glass substrate at by spray deposition technique; the structural, optical and electrical properties were studied at different NiO concentrations (0.05, 0.10 and 0.15 mol.l^{-1}). Polycrystalline NiO films with a cubic structure with a strong (111) preferred orientation were observed at all sprayed films with minimum crystallite size of 11.97 nm was attained of deposited film at 0.1 mol.l^{-1}. However, α-Ni(OH)$_2$ was observed at 0.15 mol.l^{-1}. The NiO thin films have good transparency in the visible region, the band gap energy varies from 3.54 to 376 eV was affected by NiO concentration, it is shown that the NiO thin film prepared at 0.05 mol.l^{-1} has less disorder with few defects. The NiO film deposited at 0.15 mol.l^{-1} has the electrical conductivity was 0.169 (Ω.cm)$^{-1}$.

Keywords: Nickel oxide; thin films; NiO concentrations; spray deposition technique

INTRODUCTION

Nickel oxide NiO is one of the parts of this family of TCO, its good adsorptive properties and chemical stability; it can be deposited onto glass, ceramics, oxides, and substrate materials of other types [1,2]. The semiconductors as oxides metallic are essential compounds for the development of the ultra-high frequencies components, gas sensors, photocatalysis, optoelectronics, lithium-ion microbatteries, enamels and cathode materials for alkaline batteries [2–5]. Among these, Nickel oxide (NiO) is a semitransparent p-type semiconducting material a large gap direct (3.6-4.0 eV), and has a wide range of applications, such as gas sensors, photocatalysis, dye-sensitized, electrochromic coatings, UV photo-detector, lightweight structural components in the aerospace, in ceramic structures, a counter electrode and anode layer of solid, counter electrodes oxide fuel cells [6–10].

Nanocrystalline NiO thin films can be produced by several techniques such as reactive evaporation, molecular beam epitaxy (MBE), magnetron sputtering technique, pulsed laser deposition (PLD), spray pyrolysis, sol–gel process, chemical vapor deposition, and electrochemical deposition [11–13]. Among these methods, the spray deposition has many advantages such as low cost, simple deposition equipment, easy fabrication of large-area

films, easier adjustment of composition, being able to carry out doping at the molecular level. Especially, are suitable for the fabrication of oxide thin films

The aim of this work is to obtain a thin film with good physical properties for gas sensing applications. The NiO thin films were deposited by spray pyrolysis technique with the organic solar heater, using this method for preservation and protection from chemicals and working outside laboratories. The organic solar heater consisted of a mirror layer inside (ITO glass) and a substrate holder; we established the substrate layer to maintain the substrate temperature using the mirror layer with a parabolic reflector. The NiO thin films can be deposited by spray pneumatic technique on a glass substrate at various NiO concentrations 0.05, 0.10 and 0.15 mol.l^{-1}. The NiO thin films were characterized by various methods likely X-ray diffraction, ultraviolet-visible spectrophotometer, and four point methods.

EXPERIMENTAL

Preparation of NiO solution

NiO solution was prepared by dissolving (0.05, 0.10 and 0.15 mol.l^{-1}) from the industrial powder of Nickel nitrate hexahydrate $Ni(NO_3)_2.6H_2O$ in the solvent containing equal volumes absolute H_2O, then have added drops of hydrochloric acid HCl stabilized (97.7% purity) as a stabilize the solution. The mixture solution was stirred and heated in increasing temperature between 25–50 °C for 3 h to yield a clear and transparent solution.

Deposition of NiO thin films

NiO thin films were sprayed on the heated glass substrates at 450°C with various concentrations by organic solar cells for 4 minutes of deposition time. On the other hand, the direct calcination of $Ni(NO_3)_2\ 6H_2O$ follows the reaction as:

$$2Ni(NO_3)6H_2O = 2Ni + 4NiO_2 + 4\ NO_2 + O_2 + 12H_2O \quad (1)$$

Characterization NiO thin films

The NiO doped ZnO thin films have been characterized to find the crystalline structure, optical transmission and electrical conductivity by X-ray diffraction (XRD Bruker AXS-8D with λ = 0.15406 nm), spectrophotometer (UV, Lambda 35 with 300–900 nm wavelength), and four point methods was measured by the keithley Model 2400 Low Voltage Source Meter instrument., respectively.

We have used the difference masse to determine the film thicknesses of NiO thin films, the film thickness measurement is about 380 nm.

RESULTS AND DISCUSSION

The effect of NiO concentration on the crystal structure and preferred orientations of the sprayed NiO thin films was characterized by the XRD technique. Figure 1 shows the XRD patterns of NiO thin films deposited with various concentrations of 0.05, 0.10 and 0.15 mol.l^{-1}. As the first result, All the films exhibited two diffraction peaks at 2θ = 37 and 44° related to (111) and (200) planes of NiO phase, indicating NiO thin films are polycrystalline cubic structure. The obtained crystalline structure of NiO thin films has a strong peak of the (111) crystal plane. It can be seen that the (111) peak of deposited NiO thin

film with 0.15 mol.l^{-1} has a higher intensity, which confirmed the improvement of the crystalline quality and the reduction of defects in the crystal structure. The inset of Figure 1 shows the variations of diffraction angle and FWHM of the (200) diffraction. The smaller diffraction angle of the position peak was obtained for 0.1 mol.l^{-1}, indicating the increase in the interplanar spacing d_{200}. However, the maximum value of the FWHM of the (200) peak measured for 0.1 mol.l^{-1}. On the other hand, we have observed at 2θ = 25° in the XRD patterns of NiO thin films a new phase, which it is related to α-Ni(OH)$_2$ due to the water solvent with preparation.

The crystallite size G of (200) diffraction peak of the NiO thin films was calculated using the Scherer's equation [14,15]:

$$G = \frac{0.9\lambda}{\beta \cos\theta} \tag{2}$$

where G is the crystallite size, λ is the wavelength of X-ray (λ = 1.5418 A°), β is the full width at half-maximum (FWHM), and θ is the angle of diffraction peak, these variations are presented in Table 1. Figure 2 shows the variations of the crystallite size and strain of the (101) diffraction peak as a function of NiO concentration. It can be seen, the crystallite size has a slight change estimated at 2 nm for 0.05 and 0.10 mol.l^{-1} (see Table 1). And when the increase of the NiO concentration from 0.1 to 0.15 mol.l^{-1}, the crystallite size greatly increased from 11.97 to 20.45 nm, which may be due to the improvement of the crystalline quality. However, we have observed that the crystallite size was related to the FWHM value, when the minimum crystallite size corresponded to the higher FWHM, and the decrease of FWHM due to the increase in the peak intensity. The strain has a minimum value at 0.1M due to the decrease in the lattice parameter of NiO.

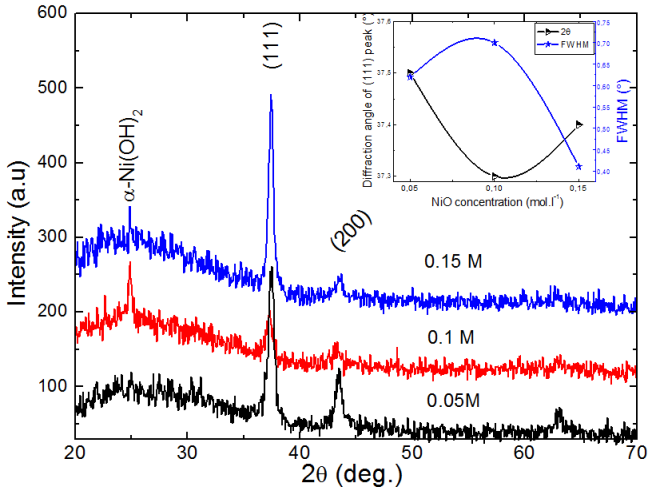


Fig. 1. X-ray diffraction spectra of NiO thin films at different NiO concentrations. The inset shows the variations of the diffraction angle and the FWHM of the (111)

Table 1. *The Diffraction angle, FWHM crystallite sizes, lattice parameter and strain of the (111) plane in NiO thin films as a function of NiO concentration*

NiO concentration (mol.l^{-1})	Diffraction angle 2θ (°)	FWHM β (deg)	Crystallite size G (nm)	Lattice parameter a (nm)	Strain ε (nm)
0.05	37.5	0.62	13.53	0.4151	0.627
0.10	37.3	0.70	11.98	0.4172	0.114
0.15	37.4	0.41	20.46	0.4161	0.371

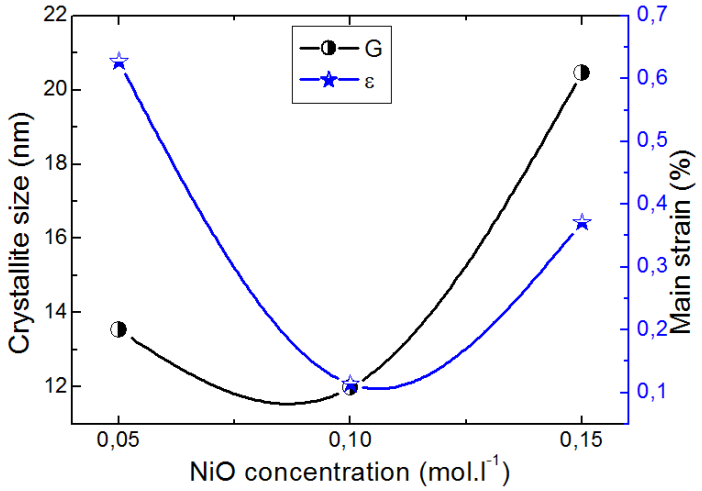


Fig. 2. The variations of the crystallite size and the strain of NiO thin films as a function of NiO concentration

The optical transmission of NiO thin films at different NiO concentrations as shown in Figure 3. As the NiO concentration increase, the transmission was decreased due to the increase in the film thickness. But the NiO thin films have a good transmission with comparing by other NiO thin films [16,17], they found that the NiO thin films have a low transmission about of 40% in the visible. The region of strong absorbance was observed between λ = 330 to 380 nm, in this region, the transmission decreased due to the excitation and the migration of the electrons from the valence band to the conduction band. It is clearly observed that the absorption edge shifted to the low wavelength can be found that the band gap was increased. The calculation of the optical band gap energy is a major factor in determining the electrical conductivity of the thin films, which based on optical transmission. It was calculated from the classical method by the extrapolation of the curve at $A = 0$ [18], which represented to the drawn of the $(A\hbar\upsilon)^2$ as a function of $h\upsilon$ (see Figure 4a) using the following equations [2,5]:

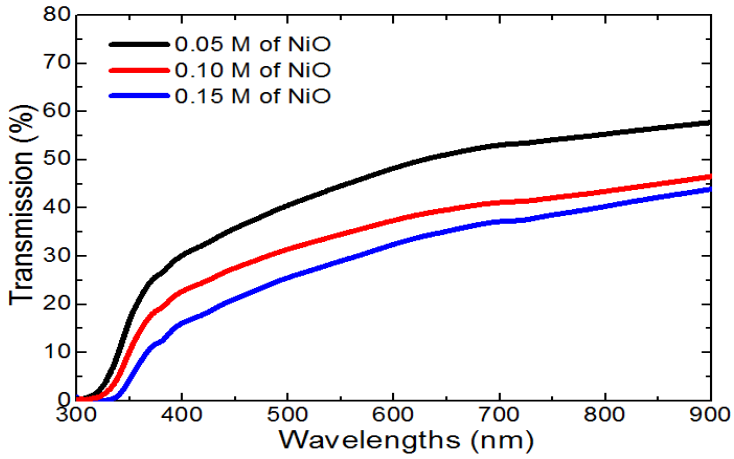


Fig. 3. Transmission spectra of NiO thin films as a function of NiO concentration

$$A = \alpha d = -\ln T \tag{3}$$

$$(A h\upsilon)^2 = C (h\upsilon - E_g) \tag{4}$$

where A is the absorbance, d is the film thickness; T is the transmission spectra of thin films; α is the absorption coefficient values; C is a constant, hυ is the photon energy and E_g the band gap energy of NiO thin films (see Table 2). On the other hand, the disorder in the NiO thin films was characterized by the Urbach energy (E_u) has been calculated by the following expression [19]:

$$A = A_0 \exp^{\left(\frac{h\upsilon}{E_u}\right)} \quad (5)$$

where A_0 a constant hυ is the photon energy and E_u is the Urbach energy, the values are presented in Table 2. Figure 4b shows the drawn of LnA as a function of photon energy hυ for deducing the Urbach energy.

Table 2. *The variation of optical band gap energy, Urbach energy and electrical conductivity as a function of NiO concentration*

NiO concentration (mol.l^{-1})	Optical gap energy E_g (eV)	Urbach energy E_u (eV)	electrical conductivity σ (nm)
0.05	3,54	0,193	0,063
0.10	3,68	0,214	0,169
0.15	3,76	0,322	0,081

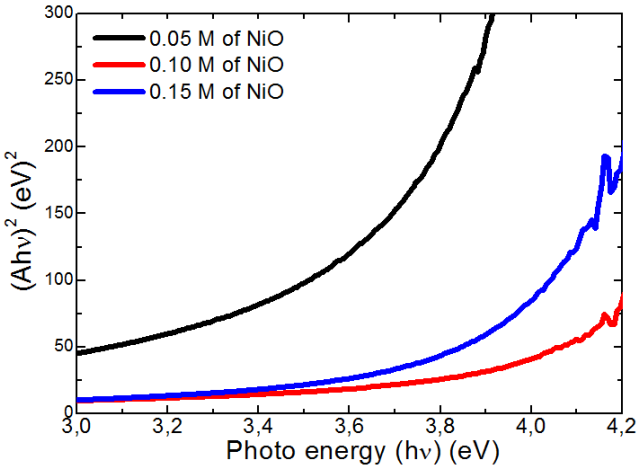


Fig. 4a. The typical variation of $(Ah\nu)^2$ vs. photon energy all deposited NiO thin film as a function of NiO concentration

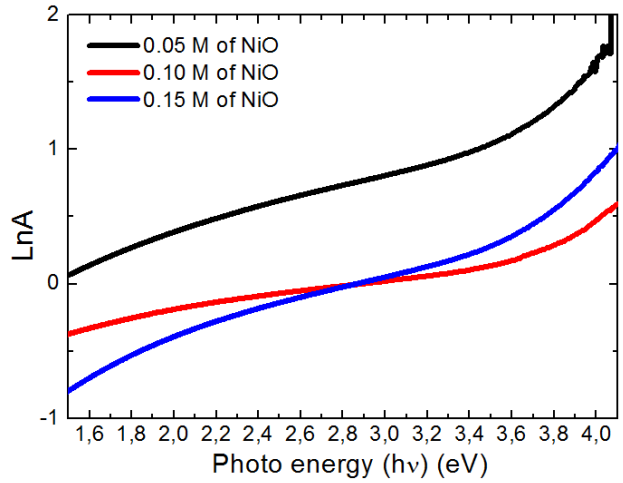


Fig. 4b. The typical variation of *LnA* vs. photon energy all deposited NiO thin film as a function of NiO concentration

Figure 5 shows the variations of optical band gap energy and Urbach energy of the NiO thin films, the variables are presented in Table 2. By an increase in the NiO concentration from 0.05 to 0.15 mol.l^{-1}, found an increase of the optical band gap with the increase of the Urbach energy. The variation of the optical band gap energy of the NiO thin films was varied from 3.5 to 3.75 eV, which is in good agreement with the E_g value of bulk NiO (3.6-4 eV) [20]. But the increase of the Urbach energy can be explained by the decrease of crystallite size and the increase of the strain was presented in Figure 2.

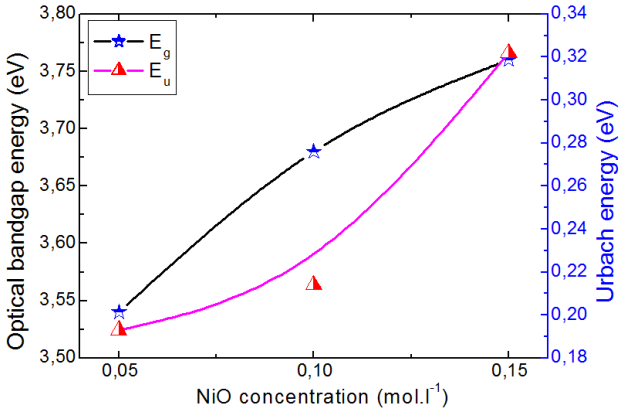


Fig. 5. The variations of optical band gap E_g and Urbach energy E_u of NiO thin films with NiO concentration

The four-point method was used to calculate the electrical conductivity σ of the NiO thin films, the measurement was based on the sheet resistance R_{sh}; it is obtained by the following relation:

$$\sigma = \frac{1}{d\mathrm{R_{sh}}} = \frac{1}{\mathrm{d}}\left(\frac{\pi}{\ln(2)}\cdot\frac{\mathrm{V}}{\mathrm{I}}\right)^{-1} \tag{6}$$

where I is the applied current = 0,5.10^{-6} and V is the measurement voltage and d is the film thickness. Figure 6 shows the variation of electrical conductivity of NiO films with different NiO concentration. As see the electrical conductivity firstly increased from 0.063 to 0.169 (Ω.cm)$^{-1}$ when NiO concentration increases from 0.05 to 0.10 mol.l^{-1}, than decreased to 0.081 (Ω.cm)$^{-1}$ at 0.15 mol.l^{-1}. As a result of the compositional changes, especially the formation of nickel vacancies, this leads to p-type conductivity. The increase in the electrical conductivity variation with NiO concentration can be explained by the decrease of crystallite size (see Figure 2).

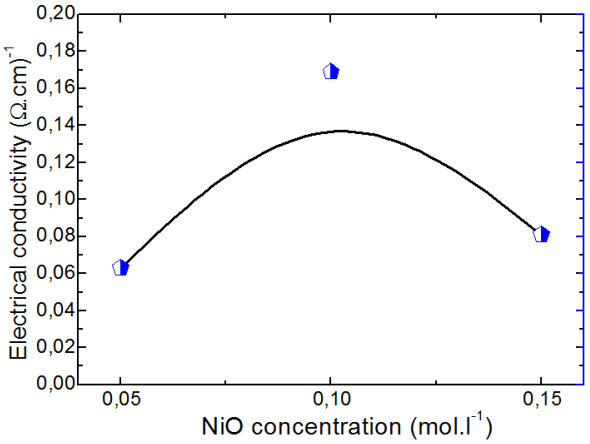


Fig. 6. Electrical conductivity of NiO thin films at different NiO concentrations

Table 3 presents the comparative results of our work with other researches; we have compared the structural, optical and electrical properties of the nickel oxide thin films. Through these results, it is clear to us that the best values for nickel oxide have been found, which are represented in the crystallite size, optical band gap, Urbach energy and electrical conductivity.

Table 3. *The comparative study of the structural, optical and electrical properties of nickel oxide thin films at different conditions*

NiO concentration ($mol.l^{-1}$)	Dep. temp T (°C)	Deposition method	Texture	Lattice parameter a (nm)	Crystallite size G (nm)	Optical energy E_g (eV)	Urbach energy E_u (eV)	Electrical conductivity σ (Ω.cm)	Rf.
3%Cu:NiO	300	RF sputtering	Crystalline	0.4208	4.0	3.8835	-	-	[8]
0.10	350	Spray pyrolysis	Crystalline	0.416	5-12	3.10	-	0.035	[15]
0.10	390			0.416	8-13	3.85	-	0.025	
0%Na:NiO	420	Spray pneumatic	Crystalline	0.4138	16.47	3.62	0.422	-	[18]
3%Na:NiO				0.4166	18.90	3.60	0.312		
0.05	350	Spray pyrolysis	Crystalline	0.417	45	3.83	-	-	[20]
0.01	250	Hydrothermal	Crystalline	0.418	6.6	3.1	-	-	[21]
Oxygen flowrate (sccm)	RT	magnétron sputtering	Crystalline	0.4205	8.45	3.41	-	5.10^{-3}	[22]
0.05	450	Spray pyrolysis	Crystalline	0.193	13.53	3.54		0.063	This work
0.10				0.214	11.98	3.68		0.169	
0.15				0.322	20.46	3.76		0.081	

CONCLUSIONS

In summary, the NiO thin films were deposited on the glass substrate by spray pneumatic technique on a glass substrate. The effect NiO concentration (0.05, 0.10 and 0.15 $mol.l^{-1}$) on structural, optical and electrical properties was investigated. Polycrystalline NiO films with a cubic structure with a strong (111) preferred orientation were observed at all sprayed films with minimum crystallite size of 11.97 nm was attained of sprayed film at 0.1 $mol.l^{-1}$. However, α-$Ni(OH)_2$ was observed at 0.15 $mol.l^{-1}$. The NiO thin films have good transparent in the visible region, the band gap energy varies from 3.54 to 376 eV was affected by NiO concentration, it is shown that the NiO thin film prepared at 0.05 $mol.l^{-1}$ has less disorder with few defects. The NiO film deposited at 0.15 $mol.l^{-1}$ has the electrical conductivity was 0.169 $(\Omega.cm)^{-1}$.

REFERENCES

1. Gund G.S., Lokhande C.D., Park H.S., Controlled synthesis of hierarchical nanoflake structure of NiO thin film for supercapacitor application, Journal of Alloys and Compounds 741 (2018) 549-556.
2. Aoun Y., Meneceur R., Benramache S., Maaoui B., Sprayed NiO-Doped p-Type Transparent ZnO Thin Films Suitable for Gas-Sensing Devices, Physics of the Solid State 62 (1) (2020) 131–136.
3. Raza M.H., Movlaee K., Wu Y., El-Refaei S.M., Karg M., Leonardi S.G., Neri G., Pinna N., Tuning the NiO Thin Film Morphology on Carbon Nanotubes by Atomic Layer Deposition for Enzyme-Free Glucose Sensing, ChemElectroChem 6 (2019) 383–392.
4. Herissi L., Hadjeris L., Aida M.S., Bougdira J., Properties of (NiO) 1-x (ZnO) x thin films deposited by spray pyrolysis, Thin Solid Films 605 (2016) 116–120.
5. Guezzoun H., Benhaoua B., Benramache S., Synthesis and characterizations of nanocrystalline Na and Al codoped NiO thin films, International Journal of Integrated Engineering 12 (1) (2020) 204-209.
6. Shang Z.W., Hsu H.H., Zheng Z.W., Cheng C.H., Progress and challenges in p-type oxide-based thin film transistors, Nanotechnology Reviews 8 (2019) 422–443.
7. Hotovy I., Spiess L., Predanocy M., Rehacek V., Racko J., Sputtered nanocrystalline NiO thin films for very low ethanol detection, Vacuum 107 (2014) 129–131.
8. Manouchehri I., Mehrparvar D., Moradiana R., Gholami K., Osati T., Investigation of structural and optical properties of copper doped NiO thin films deposited by RF magnetron reactive sputtering, Optik 127 (2016) 8124–8129.
9. Garcia-Garcia F.J., Salazar P., Yubero F., González-Elipe A.R., Non-enzymatic glucose electrochemical sensor made of porous NiO thin films prepared by reactive magnetron sputtering at oblique angles, Electrochimica Acta 201 (2016) 38–44.
10. Mironova-Ulmane N., Kuzmin A., Sildos I., Puust L., Grabis J., Magnon and Phonon Excitations in Nanosized NiO, Latvian Journal of Physics and Technical Sciences 56 (2019) 726–737.
11. Manouchehri I., Mehrparvar D., Moradian R., Gholami K., Osati T., Investigation of structural and optical properties of copper doped NiO thin films deposited by RF magnetron reactive sputtering, Optik 127 (2016) 8124–8129.
12. Bahramian A., Eyraud M., Vacandio F., Hornebecq V., Djenizian T., Knauth P., Single-step electrodeposition of superhydrophobic black NiO thin films, Journal of Applied Electrochemistry 49 (2018) 621–629.
13. Khalaf M.M., Hany M., El-Lateef Abd, Corrosion protection of mild steel by coating with TiO2 thin films co-doped with NiO and ZrO_2 in acidic chloride environments, Materials Chemistry and Physics 177 (2016) 250–265.
14. Diha A., Benramache S., Fellah L., The Crystalline Structure, Optical and Conductivity Properties of Fluorine Doped ZnO Nanoparticles, Journal of Nano and Electronic Physics 11 (2019) 03002.
15. Varughese G., Rini V., Suraj S.P., Usha K.T., Characterisation and Optical Studies of Copper Oxide Nanostructures Doped with Lanthanum Ions, Advances in Materials Science 14 (2014) 59–60
16. Kate R.S., Bulakhe S.C., Deokate R.J., Effect of Substrate Temperature on Properties of Nickel Oxide (NiO) Thin Films by Spray Pyrolysis, Journal of Electronic Materials 48 (2019) 3220–3228.

17. Panneerselvam V., Chinnakutti K.K., Salammal S.T., Soman A.K., Parasuraman K., Vishwakarma V., Kanagasabai V., Role of copper/vanadium on the optoelectronic properties of reactive RF magnetron sputtered NiO thin films, Applied Nanoscience 8 (2018) 1299–1312.
18. Aoun Y., Marrakchi M., Benramache S., Benhaoua B., Lakel S., Cheraf A., Preparation and Characterizations of Monocrystalline Na Doped NiO Thin Films, Materials Research 21 (2018) e20170681.
19. Benramache S., Aoun Y., Lakel S., Mourghade H., Gacem R., Benhaoua B., Effect of Annealing Temperature on Structural, Optical and Electrical Properties of ZnO Thin Films Prepared by Sol-Gel Method, Journal of Nano- and Electronic Physics 10(6) (2018) 06032.
20. Mahmoud S.A., Alshomer S., Tarawnh M.A., Structural and optical dispersion characterisation of sprayed nickel oxide thin films, Journal of Modern Physics 2(2011) 1178-1186.
21. Nakate U.T., Ahmad R., Patil P., Yu Y.T., Hahn Y.B., Ultra thin NiO nanosheets for high performance hydrogen as sensor device, Applied Surface Science 506 (2020) 144971.
22. Salunkhe P., Ali M. A.V., Kekuda D., Investigation on tailoring physical properties of Nickel Oxide thin films grown by dc magnetron sputtering, Materials Research Express 7 (2020) 016427.